International Journal of Modern Physics D
(2020) 2050005 (13 pages)

DOI: 10.1142/S0218271820500054

Higgs vacuum decay in a braneworld

Leopoldo Cuspinera[*,¶], Ruth Gregory[*,†,‡,‖], Katie M. Marshall[§,**]
and Ian G. Moss[§,††]

[*]*Department of Physics,*
Institute for Particle Physics Phenomenology,
Durham University, South Road, Durham DH1 3LE, UK

[†]*Department of Mathematical Sciences,*
Durham University, South Road, Durham DH1 3LE, UK

[‡]*Perimeter Institute, 31 Caroline Street North,*
Waterloo, ON N2L 2Y5, Canada

[§]*School of Mathematics, Statistics and Physics,*
Newcastle University, Newcastle Upon Tyne NE1 7RU, UK
[¶]*j.l.cuspinera@durham.ac.uk*
[‖]*r.a.w.gregory@durham.ac.uk*
[**]*k.marshall6@newcastle.ac.uk*
[††]*ian.moss@newcastle.ac.uk*

Received 9 August 2019
Accepted 25 October 2019
Published 4 December 2019

We examine the effect of large extra dimensions on vacuum decay in the Randall–Sundrum (RS) braneworld paradigm. We assume the scalar field is confined to the brane, and compute the probability for forming an "anti-de Sitter" (AdS) bubble inside a critical flat RS brane. We present the first full numerical solutions for the brane instanton considering two test potentials for the scalar field. We explore the geometrical impact of thin and thick bubble walls, and compute the instanton action in a range of cases. We conclude by commenting on a more physically realistic potential relevant for the Standard Model Higgs. For bubbles with large backreaction, the extra dimension has a dramatic effect on the tunnelling rate, however, for the weakly backreacting bubbles more relevant for realistic Standard Model potentials, the extra dimension has little impact.

Keywords: Vacuum decay; bubble nucleation; gravitational instantons.

1. Introduction

When Coleman and de Luccia[1] pioneered the study of vacuum decay in curved spacetime, they described the possibility as "the ultimate ecological catastrophe."

Whilst the comment was somewhat tongue in cheek, the recent measurement of the Higgs mass[2,3] and the realisation that the Standard Model Higgs field could well be in a metastable state,[4–12] has brought the catastrophe a little closer to reality! Fortunately, the timescale for decay according to Coleman *et al.*,[1,13,14] (see also Ref. 15), is sufficiently large that we would seem not be troubled, except that the Coleman results are computed in a highly symmetric background. Recent work by two of us[16–20] has argued that taking into account inhomogeneities such as primordial black holes can dramatically shorten the lifetime of the false vacuum (see also Refs. 21 and 22 for early work, and Refs. 23–26 for alternate perspectives).

Apart from primordial black holes, the other possible scenario in which small black holes might occur is in particle collisions if there are large extra dimensions. Large extra dimension scenarios were introduced initially to provide an alternate, geometric, resolution of the hierarchy problem. The idea that our four-dimensional (4D) Planck scale is derived from a higher dimensional Planck mass close to the Standard Model scale[27–30]; we then live on a 4D *brane* embedded in a higher dimensional spacetime. In such scenarios, it is easier to form black holes in particle collisions (see e.g. Refs. 31–33). Our relatively high Planck scale, $M_p^2 = 1/8\pi G_N$, is then the result of a geometric hierarchy coming from an integration over the extra dimensions.

In a previous paper,[34] we computed the probability for seeded decay with a brane black hole, following the notion that small black holes could also occur in particle collisions if there are large extra dimensions. As in the straightforward 4D case, we found the decay rate to be significantly enhanced over the Hawking evaporation rate for a range of small mass black holes. However, we did not compare the seeded nucleation process to an unseeded brane Coleman–de Luccia (CDL) equivalent rate, hence we could not clarify the extent to which enhancement of tunnelling was due to the black hole, or the extra dimensions. In this work, we address this question, and explore the vacuum decay of a brane scalar in the absence of any black hole. The instantons we will consider will be the true brane equivalents of the CDL solution. Early work on brane instantons[35,36] focussed largely on constructing the Euclidean solutions and presented results on the action within the thin wall approximation, subsequent work either focussed on compact instantons in, or near, the thin wall limit,[37] or approximate Hawking–Moss-type instantons[38] and bulk scalar instantons.[39] See also some interesting ideas on Randall–Sundrum (RS) brane decay by 5D "bubble of nothing" type processes,[40,41] as well as instantons in Dvali-Gabadadze-Porrati (DGP).[42,43]

In this paper, we consider vacuum decay of a scalar field localised on a brane embedded in a 5D anti-de Sitter (AdS) bulk. We first review the derivation of the instanton equations in Sec. 2, then present numerical solutions for the scalar CDL-equivalent brane instanton in Sec. 3. In Sec. 4, we turn to a computation of the action, showing how to renormalise the instanton action properly, and computing the action for a range of potentials and Planck mass hierarchies before concluding in Sec. 5.

2. The Instanton Equations of Motion

In the RS model, spacetime is 5D with a negative cosmological constant living in the bulk. This negative curvature of spacetime causes a localisation of the graviton on the brane, the background solution being a brane with energy and tension equal and precisely tuned to the bulk cosmological constant, giving a flat brane at $z = 0$:

$$ds^2 = e^{-2|z|/\ell}\eta_{\mu\nu}dx^\mu dx^\nu - dz^2, \tag{2.1}$$

where $\ell^2 = -6/\Lambda_5$ is the AdS curvature scale and $\eta_{\mu\nu}$ the Minkowski metric. The local negative curvature of the bulk supports the brane tension σ that is easily calculated from the Israel junction conditions[44]:

$$\mathcal{K}^{(+)}_{\mu\nu} = -\frac{1}{\ell}\eta_{\mu\nu} \Rightarrow \mathcal{K}^{+}_{\mu\nu} - \mathcal{K}^{+}\eta_{\mu\nu} = \frac{3}{\ell}\eta_{\mu\nu} = 4\pi G_5\sigma\eta_{\mu\nu}. \tag{2.2}$$

One can add energy momentum to the brane, for example a "brane cosmological constant," so that σ is greater or less than the critical value,[45–51] a cosmological fluid, or a perturbative localised source. In all cases, the intuitive visualisation of brane matter is that it causes the braneworld to bend as first pointed out by Garriga and Tanaka[52] (see also Refs. 53 and 54).

We are interested here in pure false vacuum decay, i.e. the brane equivalent of a CDL instanton that is a Euclidean solution to the Einstein plus brane scalar field equations that has $O(4)$ symmetry on the brane. This level of symmetry is mathematically equivalent to a cosmological braneworld solution: there is a brane coordinate τ upon which the brane solution depends, and a coordinate that tracks the warping in the bulk. If we assume that the full brane plus bulk solution also has $O(4)$ symmetry, then a "generalised Birkhoff theorem" applies,[50] and the bulk equations of motion can be fully integrated with the brane now following a trajectory in the bulk consistent with the local energy–momentum of the instanton solution (for proof see Refs. 35, 36 and 50).

To find these equations of motion, we take a simple scalar field Lagrangian on the brane in the Wick-rotated Euclidean signature geometry:

$$\mathcal{L}_\phi = \frac{1}{2}g^{\mu\nu}\phi_{,\mu}\phi_{,\nu} + V(\phi). \tag{2.3}$$

The general bulk admitting an $O(4)$ symmetric brane solution is a Schwarzschild-AdS black hole,[35,50] however, as we are computing the brane equivalent of the CDL instanton, we will take the pure AdS_5 spacetime in the bulk

$$ds^2_{\text{bulk}} = h(r)dt^2 + \frac{dr^2}{h(r)} + r^2 d\Omega^2_{\text{III}}, \quad h(r) = 1 + \frac{r^2}{\ell^2} \tag{2.4}$$

as a bulk black hole induces a cosmological radiation source on the brane.[49–51]

The brane traces out a submanifold in (2.4) that can be parametrised by intrinsic coordinates $\{\tau, \theta^\alpha\}$ $(\alpha = 1, 2, 3)$:

$$X^\mu = (t(\tau), a(\tau), \theta^\alpha), \tag{2.5}$$

where τ is chosen to be the proper time parameter on the brane and $a(\tau)$ the radial trajectory of the brane.

$$h\dot{t}^2 + \frac{\dot{a}^2}{h} = 1, \tag{2.6}$$

so that the induced brane metric is identical to the CDL geometry:

$$ds^2_{\text{brane}} = d\tau^2 + a^2(\tau) d\Omega^2_{\text{III}}. \tag{2.7}$$

The scalar field depends only on τ, and the energy–momentum is readily found to be

$$\begin{aligned} T_{\tau\tau} &= \sigma + V - \frac{1}{2}\dot{\phi}^2 = \frac{3\mathcal{E}}{4\pi G_5}, \\ T_{\alpha\beta} &= \left[\sigma + V + \frac{1}{2}\dot{\phi}^2\right] g_{\alpha\beta} = \frac{3\mathcal{T}}{4\pi G_5} g_{\alpha\beta}, \end{aligned} \tag{2.8}$$

that sources the brane trajectory.

The Israel junction equations are then

$$\begin{aligned} K^+_{\tau\tau} &= \frac{1}{h\dot{t}}\left(\ddot{a} - \frac{h'(r)}{2}\right) = 2\mathcal{E} - 3\mathcal{T}, \\ K^+_{\alpha\beta} &= -\frac{\dot{t}h}{a} g_{\alpha\beta} = -\mathcal{E} g_{\alpha\beta}, \end{aligned} \tag{2.9}$$

usually expressed in the cosmological format of Friedmann and conservation of energy–momentum equations:

$$\begin{aligned} \left(\frac{\dot{a}}{a}\right)^2 &= \frac{1}{a^2} + \frac{1}{\ell^2} - \mathcal{E}^2, \\ 0 &= \dot{\mathcal{E}} + \frac{3\dot{a}}{a}(\mathcal{E} - \mathcal{T}). \end{aligned} \tag{2.10}$$

For numerical integration of the scalar field, it is more useful to use the Raychaudhuri equation, and substituting in the form of the energy–momentum (2.8) we finally arrive at the full set of brane scalar instanton equations:

$$\begin{aligned} \left(\frac{\dot{a}}{a}\right)^2 &= \frac{1}{a^2} - \frac{8\pi G_N}{3}\left(V - \frac{1}{2}\dot{\phi}^2\right) - \left(\frac{4\pi G_N \ell}{3}\right)^2 \left(V - \frac{1}{2}\dot{\phi}^2\right)^2, \\ \frac{\ddot{a}}{a} &= -\frac{8\pi G_N}{3}(V + \dot{\phi}^2) - \left(\frac{4\pi G_N \ell}{3}\right)^2 \left(V - \frac{1}{2}\dot{\phi}^2\right)\left(V + \frac{5}{2}\dot{\phi}^2\right), \\ \ddot{\phi} + \frac{3\dot{a}}{a}\dot{\phi} &= \frac{\partial V}{\partial \phi}, \end{aligned} \tag{2.11}$$

where we have substituted the Newton constant $G_N = G_5/\ell$ in the gravitational coupling. These are precisely the Shiromizu–Maeda–Sasaki[53] equations with vanishing Weyl term, also analysed in Ref. 38 for the Hawking–Moss case. As ℓ drops,

gravity becomes more strongly localised on the brane, hence the 4D limit is $\ell \to 0$, and (2.11) become the 4D instanton equations.

It is also worth noting that the critical RS brane (with $V = \dot{\phi} = 0$) has $\dot{a} \equiv 1$. This leads to the brane trajectory

$$r = a(\tau) = \tau, \quad t(\tau) = \frac{\ell}{2} \log\left(1 + \frac{\tau^2}{\ell^2}\right) \tag{2.12}$$

in terms of the original coordinates (2.4). This is a less familiar form for the critical RS brane, obtained because we are solving for the brane in bulk global coordinates, rather than the usual Poincaré patch. The trajectory can easily be transformed to its familiar form using

$$e^{z/\ell} = \frac{e^{t/\ell}}{\sqrt{1 + \dfrac{r^2}{\ell^2}}}, \quad x^i = e^{z/\ell} r n_4^i, \tag{2.13}$$

where n_4 is the unit vector in four dimensions.

3. The Scalar Brane Instanton

In order to investigate vacuum decay, we use two basic model scalar potentials. The first is a standard quartic potential V_q, with a potential barrier between a false and true vacuum. It is convenient to parametrise this potential with the value of $\phi = \phi_M$ at the maximum and $\phi = \phi_V$ at the global minimum:

$$V_q(\phi) = g\left[\frac{\phi^4}{4} - \frac{\phi^3}{3}(\phi_V + \phi_M) + \frac{\phi^2}{2}\phi_V\phi_M\right]. \tag{3.1}$$

The potential vanishes at the false vacuum $\phi = 0$ and the value at the true vacuum is

$$V_q(\phi_V) = \frac{g}{12}\phi_V^3(2\phi_M - \phi_V). \tag{3.2}$$

Note that since we require $V_q(\phi_V) < 0$, $\phi_V > 2\phi_M$.

The second potential we wish to investigate, V_h, more closely approximates the Higgs potential. The form of this potential has one local minimum and a barrier, where on the far side the potential does not turn up again until it reaches very high field values. This allows for the possibility of a phase transition and the nucleation of a true vacuum bubble. The potential takes the form

$$V_h(\phi) = \frac{1}{4}\lambda_{\text{eff}}(\phi)\phi^4, \tag{3.3}$$

where the effective coupling

$$\lambda_{\text{eff}} = g\left\{\left(\ln\frac{\phi}{M_p}\right)^4 - \left(\ln\frac{\Lambda}{M_p}\right)^4\right\}. \tag{3.4}$$

$g \sim 10^{-5}$ is a constant that can be used to tune to the potential to closely fit the Standard Model Higgs potential.

In each case, we integrate (2.11) from the centre of the instanton, $\tau = 0$, looking for a solution that asymptotes the flat critical RS trajectory (2.12). However, note that because we set boundary conditions at $\tau = 0$ of $a = 0$, $\dot{a} = 1$ and $\dot{\phi} = 0$, the flat geometry at large τ is $\phi \to \phi_{\rm FV}$, the value of ϕ in the false vacuum, $a \to \tau + c$ — integrating through the bubble wall produces an offset in the value of r relative to t. While this is not particularly relevant to the form of the bubble solution, for which $a(\tau)$ is important, it is a crucial observation for the computation of the action, as we will return to in Sec. 4.

The quadratic potential (3.1) is particularly useful for exploring the variation from thin to thick bubble walls, and for varying backreaction strengths. To illustrate this, we present results for two representative potentials, one giving a strongly backreacting thin wall, with parameter values $g = 1, \phi_V = M_p, \phi_M = 0.4M_p$, and the other a weakly backreacting thick wall with parameter values $g = 1/2, \phi_V = M_p, \phi_M = 0.1M_p$; in both cases the Planck scales are $M_5 = 0.4$, $M_p = 1$, hence the bulk AdS lengthscale is $\ell = 1/M_5^3 = 125/8$. Figure 1 shows the potential V_q for these two choices of parameters; note the thin wall potential (shown in blue) has a significant potential barrier between the vacua, but less well represents a Higgs-type potential, whereas the thick wall potential (shown in red) more closely resembles the Higgs potential, having a very small barrier relative to the global minimum.

The scalar field solution is shown in Fig. 2, and demonstrates clearly the distinction between the potentials: the thin wall has a clear, sharp transition from false to true vacuum around $\tau \sim 25$, whereas the thick wall does not even reach the true vacuum by the centre of the bubble. The effect of the bubble on the embedding of the brane is shown in Fig. 3. The strongly backreacting thin wall brane shows the transition between the flat RS critical asymptotic false vacuum brane, and the sub-critical true vacuum AdS embedding in the interior of the brane. The weakly interacting thick wall has a much less significant displacement, and does not reach the spherical shape of the sub-critical brane.

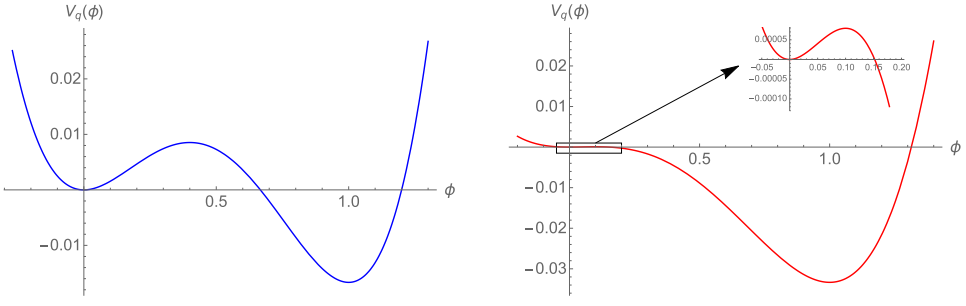

Fig. 1. (Colour online) The V_q potentials referred to in the text. On the left in blue with $\phi_M = 0.4$, and $\phi_V = 1$ (with $M_p = 1$), corresponding to a well-defined bubble wall. On the right in red the potential more closely approximated the Higgs potential, with $\phi_M = 0.1$, and corresponds to a thick wall bubble.

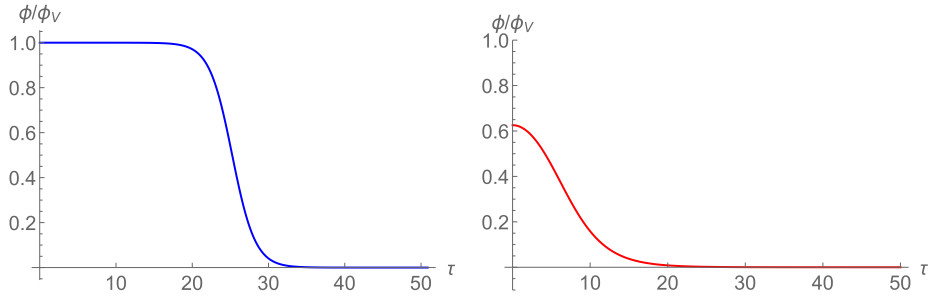

Fig. 2. (Colour online) The scalar field solution for the potentials shown in Fig. 1. Once again, blue corresponds to the thin wall bubble, here clearly seen as a step in ϕ, and red to the thick wall bubble.

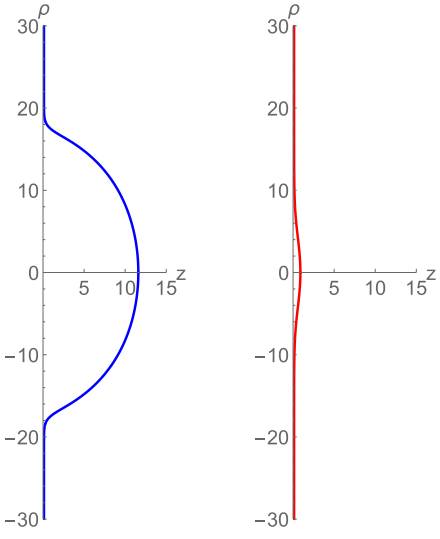

Fig. 3. (Colour online) The geometry of the brane with bubble embedding shown in Poincaré coordinates, as is usual for the flat RS brane. (Colour scheme as Fig. 1.)

4. Computation of the Action

Having found the Euclidean brane bubble solutions, we now need to compute their action, in order to find the leading order exponential behaviour of the tunnelling probability. We first derive the action for a general brane scalar solution, given a large r cutoff, then discuss the proper background subtraction. The Euclidean action is given by

$$S = \frac{1}{8\pi G_5}\int_{M^+} d^5x(-R_5 + 2\Lambda_5) + \int_{\partial M^+} d^4x\left[\frac{2K}{8\pi G_5} + \frac{1}{2}(\partial\phi)^2 + V + \sigma\right]$$
$$= \int_{M^+}\frac{d^5x}{\pi G_5\ell^2} + \int_{\partial M^+} d^4x\left[\frac{\dot{\phi}^2}{6} - \frac{1}{3}(V+\sigma)\right] \tag{4.1}$$

that is formally infinite for the background false vacuum critical brane solution. Note that this action is written in the Gibbons–Hawking boundary format, with the brane being a boundary of a 5D manifold, the normal n_μ pointing in to the manifold — this expression manifestly includes the $\mathbb{Z}_2$ symmetry of the brane.

In order to find the instanton action, we first apply a cutoff well outside the radius of the bubble. We define the cutoff by $a(\tau_R) = R$, and bound the bulk coordinates by $r \leq R$, and $t \leq t_b(\tau_R)$, where t_b is the value of t on the brane found by integrating the relation (4.3). Note that t is also bounded below by $t_b(0)$. We obtain

$$S_R = \frac{2\pi}{G_5 \ell^2} \int_{t_b(0)}^{t_b(R)} dt \int_0^R dr r^3 + 2\pi^2 \int_0^{\tau_R} d\tau a^3(\tau) \left[\frac{\dot{\phi}^2}{6} - \frac{1}{3}(V + \sigma) \right]. \tag{4.2}$$

Now, whereas the bulk integral is naturally expressed in terms of the bulk coordinates t and r, the brane integral and the instanton solution are naturally expressed in terms of the intrinsic coordinate τ. While we can easily identify $r = a(\tau)$, the relation to the bulk time coordinate is differential:

$$\frac{dt}{d\tau} = \frac{\mathcal{E} a(\tau)}{1 + \dfrac{a^2}{\ell^2}}. \tag{4.3}$$

Using this relation, we can rearrange the bulk integral, integrating first with respect to r, then translating to a τ integral to finally obtain

$$S_R = \frac{\pi^2}{3} \int_0^{\tau_R} d\tau \frac{a^3}{1 + \dfrac{a^2}{\ell^2}} [\dot{\phi}^2 - 2V - 2\sigma], \tag{4.4}$$

where τ_R is defined as $a(\tau_R) = R$. This integral now is in a simple "brane" format, and we can easily insert in the solutions of the scalar instanton equations. The integral diverges as τ_R^2 for large $R \sim \tau_R$, however, outside the bubble, both instanton and false vacuum branes are identical, thus once we subtract the background false vacuum action this divergence will be removed.

To subtract the background false vacuum a crucial observation is that the false vacuum action is *not* obtained simply by deleting all but the σ term in (4.4), since not only is $a(\tau)$ different, but also the value of τ at which the brane radius becomes equal to R (see Fig. 4). We must therefore perform one final manipulation to get the instanton action. The critical false vacuum brane action is

$$S_{\mathrm{FV}} = \frac{-2\pi^2}{3} \int_0^{\tau_R'} \frac{a^3(\tau') \sigma d\tau'}{1 + \dfrac{a^2(\tau')}{\ell^2}} = \frac{-2\pi^2}{3} \int_0^R \frac{a^3 \sigma da}{1 + \dfrac{a^2}{\ell^2}} \tag{4.5}$$

but now that this is expressed as an integral over a, we can compare this to the a integral for the bubble:

$$S_{\mathrm{bub}} = \frac{\pi^2}{3} \int_0^R \frac{da}{\dot{a}} \frac{a^3}{1 + \dfrac{a^2}{\ell^2}} [\dot{\phi}^2 - 2V - 2\sigma] \tag{4.6}$$

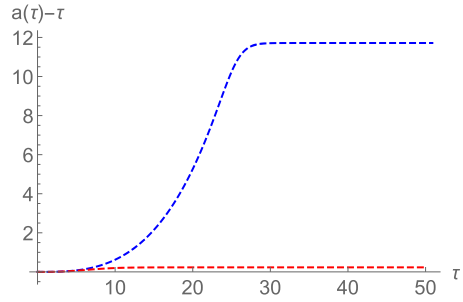

Fig. 4. (Colour online) The offset between a and τ for the thin and thick wall. (Colour scheme as Fig. 1.)

and using this expression gives the final subtracted action for the instanton as

$$B = S_R - S_{\rm FV} = \frac{2\pi^2}{3}\int_0^R \frac{da}{\dot{a}}\frac{a^3}{1+\dfrac{a^2}{\ell^2}}\left[\frac{\dot{\phi}^2}{2} - V + (\dot{a}-1)\sigma\right]$$

$$= \frac{2\pi^2}{3}\int_0^{\tau_R} d\tau \frac{a^3}{1+\dfrac{a^2}{\ell^2}}\left[\frac{\dot{\phi}^2}{2} - V + (\dot{a}-1)\sigma\right] \qquad (4.7)$$

now expressed as an integral over the brane time-coordinate (and numerical integration parameter) τ. This action can now be exponentiated to give the dominant contribution to the probability of vacuum decay.

Figure 5 shows the tunnelling exponent for the potential V_q with the parameter sets considered in Sec. 3, these are plotted as a function of the mass parameter $M_5 = M_p^{2/3}\ell^{-1/3}$, which determines the strength of gravity in five dimensions. The

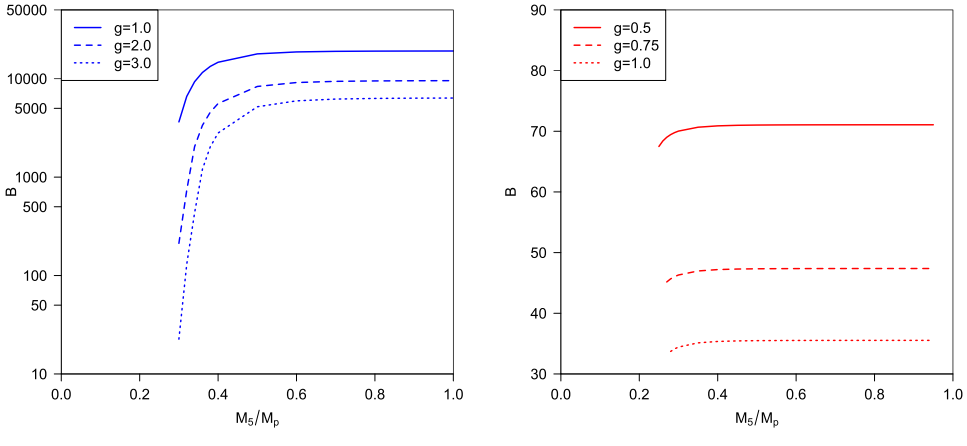

Fig. 5. The vacuum decay exponent B for the quadratic potential plotted as a function of M_5 for barriers with $\phi_M = 0.4M_p$ (left) and $\phi_M = 0.1M_p$ (right). The exponent approaches the 4D value as M_5 approaches the 4D Planck mass M_p.

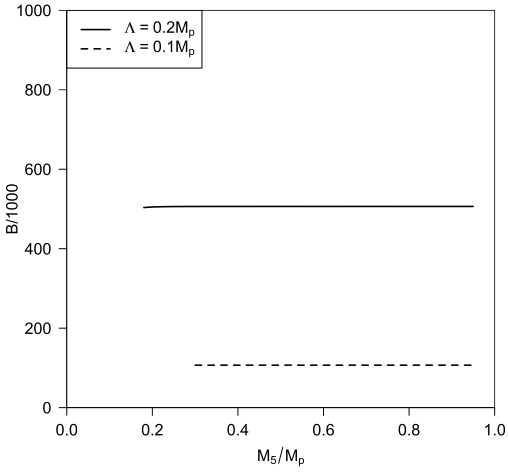

Fig. 6. The vacuum decay exponent B plotted as a function of M_5 for Higgs potentials with a range of values or the instability scale Λ. There is no dependence on the extra dimension.

barrier is at $\phi_M = 0.4M_p$ and $\phi_M = 0.1M_p$. These test case examples show a reduction in B, hence an increase in the vacuum decay rate, due to the increasing influence of the extra dimension.

The edge of the plots denotes a minimum value of M_5 beyond which the numerical solutions cease to exist. Close to this limit, the total surface tension on the brane becomes negative near the centre of the bubble. Note that the allowed range of M_5 is narrow, as in the examples plotted above, therefore does not correspond to a significant hierarchy. Therefore adding an extra dimension only affects the decay rate in very specialised situations.

We also show the tunnelling exponent for the Higgs-style potential V_H, with parameters chosen within the Standard Model range in Fig. 6. The Higgs potential is small at the Planck scale because the parameter g in the potential is small. Consequently, vacuum decay rates with the Higgs potential show no obvious dependence on the extra dimensions.

5. Summary

To sum up: we have found instanton solutions for a brane scalar field representing vacuum decay from a critical RS flat brane. We explored general bubble solutions, as well as an approximate Higgs potential. We calculated the tunnelling exponent for a range of warping in the extra dimension, and compared it to that of a phase transition in 4D asymptotically flat space. The influence of the fifth dimension on tunnelling rates is relatively minor, except for a strongly backreacting bubble.

A Higgs-style potential was also considered, however, for realistic parameter ranges, the impact of the extra dimension was negligible. This is to be contrasted to the case of vacuum decay seeded by primordial brane black holes, as in Ref. 34,

where the decay rate is significant. We conclude that, rather like the 4D case, black holes are required to produce significant decay rates.

One interesting feature of our numerical solutions was that they had a sharp cut-off in the allowed value of M_5, due to the brane tension becoming negative. This is possibly due to the fact we integrate out from $\tau = a = 0$, hence this method does not allow for a wormhole-type solution where the brane transitions from positive to negative tension as in Refs. 40 and 41. It might be interesting to consider this further.

Acknowledgments

We are grateful for the hospitality of the Perimeter Institute, where part of this research was undertaken. This work was supported in part by the Leverhulme grant *Challenging the Standard Model with Black Holes* and in part by STFC consolidated grant ST/P000371/1. LC acknowledges financial support from CONACyT, RG is supported in part by the Perimeter Institute for Theoretical Physics, and KM is supported by an STFC studentship. Research at Perimeter Institute is supported by the Government of Canada through the Department of Innovation, Science and Economic Development Canada and by the Province of Ontario through the Ministry of Research, Innovation and Science.

References

1. S. Coleman and F. de Luccia, *Phys. Rev. D* **21** (1980) 3305.
2. ATLAS Collab. (G. Aad *et al.*), *Phys. Lett. B* **710** (2012) 49, arXiv:1202.1408 [hep-ex].
3. CMS Collab. (S. Chatrchyan *et al.*), *Phys. Lett. B* **710** (2012) 26, arXiv:1202.1488 [hep-ex].
4. G. Degrassi, S. Di Vita, J. Elias-Miro, J. R. Espinosa, G. F. Giudice, G. Isidori and A. Strumia, *J. High Energy Phys.* **1208** (2012) 098, arXiv:1205.6497 [hep-ph].
5. A. Gorsky, A. Mironov, A. Morozov and T. N. Tomaras, *J. Exp. Theor. Phys.* **120** (2015) 399 (*Zh. Eksp. Teor. Fiz.* **147** (2015) 399), arXiv:1409.0492 [hep-ph].
6. F. Bezrukov and M. Shaposhnikov, *Zh. Eksp. Teor. Fiz.* **147** (2015) 389, arXiv:1411.1923 [hep-ph].
7. J. Ellis, arXiv:1501.05418 [hep-ph].
8. K. Blum, R. T. D'Agnolo and J. Fan, arXiv:1502.01045 [hep-ph].
9. I. V. Krive and A. D. Linde, *Nucl. Phys. B* **432** (1976) 265.
10. M. S. Turner and F. Wilczek, *Nature D* **79** (1982) 633.
11. M. Sher, *Phys. Rep.* **179** (1989) 273.
12. G. Isidori, G. Ridolfi and A. Strumia, *Nucl. Phys. B* **609** (2001) 387, arXiv:hep-ph/0104016.
13. S. Coleman, *Phys. Rev. D* **15** (1977) 2929.
14. C. G. Callan and S. Coleman, *Phys. Rev. D* **16** (1977) 1762.
15. I. Y. Kobzarev, L. B. Okun and M. B. Voloshin, *Sov. J. Nucl. Phys.* **20** (1975) 644 (*Yad. Fiz.* **20** (1974) 1229).
16. R. Gregory, I. G. Moss and B. Withers, *J. High Energy Phys.* **1403** (2014) 081, arXiv:1401.0017 [hep-th].
17. P. Burda, R. Gregory and I. Moss, *Phys. Rev. Lett.* **115** (2015) 071303, arXiv:1501.024937 [hep-th].

18. P. Burda, R. Gregory and I. Moss, *J. High Energy Phys.* **1508** (2015) 114, arXiv:1503.07331 [hep-th].
19. P. Burda, R. Gregory and I. Moss, *J. High Energy Phys.* **1606** (2016) 025, arXiv:1601.02152 [hep-th].
20. R. Gregory and I. G. Moss, The fate of the higgs vacuum, in *PoS ICHEP*, Vol. 2016 (2016) 344 p., arXiv:1611.04935 [hep-th].
21. W. A. Hiscock, *Phys. Rev. D* **35** (1987) 1161.
22. V. Berezin, V. Kuzmin and I. Tkachev, *Phys. Lett. B* **207** (1988) 397.
23. N. Tetradis, *J. Cosmol. Astropart. Phys.* **1609** (2016) 036, arXiv:1606.04018 [hep-ph].
24. P. Chen, G. Domènech, M. Sasaki and D.-H. Yeom, *J. High Energy Phys.* **1707** (2017) 134, arXiv:1704.04020 [gr-qc].
25. D. Gorbunov, D. Levkov and A. Panin, *J. Cosmol. Astropart. Phys.* **1710** (2017) 016, arXiv:1704.05399 [astro-ph.CO].
26. K. Mukaida and M. Yamada, *Phys. Rev. D* **96** (2017) 103514, arXiv:1706.04523 [hep-th].
27. N. Arkani-Hamed, S. Dimopoulos and G. R. Dvali, *Phys. Lett. B* **429** (1998) 263, arXiv:hep-ph/9803315.
28. I. Antoniadis, N. Arkani-Hamed, S. Dimopoulos and G. R. Dvali, *Phys. Lett. B* **436** (1998) 257, arXiv:hep-ph/9804398.
29. L. Randall and R. Sundrum, *Phys. Rev. Lett.* **83** (1999) 3370, arXiv:hep-ph/9905221.
30. L. Randall and R. Sundrum, *Phys. Rev. Lett.* **83** (1999) 4690, arXiv:hep-th/9906064.
31. S. Dimopoulos and G. L. Landsberg, *Phys. Rev. Lett.* **87** (2001) 161602, arXiv:hep-ph/0106295.
32. S. B. Giddings and S. D. Thomas, *Phys. Rev. D* **65** (2002) 056010, arXiv:hep-ph/0106219.
33. G. L. Landsberg, *Eur. Phys. J. C* **33** (2004) S927, arXiv:hep-ex/0310034.
34. L. Cuspinera, R. Gregory, K. Marshall and I. G. Moss, *Phys. Rev. D* **99** (2019) 024046, arXiv:1803.02871 [hep-th].
35. R. Gregory and A. Padilla, *Phys. Rev. D* **65** (2002) 084013, arXiv:hep-th/0104262.
36. R. Gregory and A. Padilla, *Class. Quantum Grav.* **19** (2002) 279, arXiv:hep-th/0107108.
37. S. C. Davis and S. Brechet, *Phys. Rev. D* **71** (2005) 104023, arXiv:hep-ph/0503243.
38. M. Demetrian, *Gen. Relativ. Gravit.* **38** (2006) 953, arXiv:gr-qc/0506028.
39. E. Dudas, J. Mourad and F. Nitti, *J. High Energy Phys.* **0708** (2007) 057, arXiv:0706.1269 [hep-th].
40. D. Ida, T. Shiromizu and H. Ochiai, *Phys. Rev. D* **65** (2002) 023504, arXiv:hep-th/0108056.
41. H. Ochiai, D. Ida and T. Shiromizu, *Prog. Theor. Phys.* **107** (2002) 703, arXiv:hep-th/0111070.
42. K. Izumi, K. Koyama, O. Pujolas and T. Tanaka, *Phys. Rev. D* **76** (2007) 104041, arXiv:0706.1980 [hep-th].
43. F. Sbisà and K. Koyama, *J. Cosmol. Astropart. Phys.* **1406** (2014) 029, arXiv:1404.0712 [hep-th].
44. W. Israel, *Nuovo Cimento* **B44** (1966) 4349.
45. H. A. Chamblin and H. S. Reall, *Nucl. Phys. B* **562** (1999) 133, arXiv:hep-th/9903225.
46. N. Kaloper, *Phys. Rev. D* **60** (1999) 123506, arXiv:hep-th/9905210.
47. P. Kraus, *J. High Energy Phys.* **9912** (1999) 011, arXiv:hep-th/9910149.
48. A. Karch and L. Randall, *J. High Energy Phys.* **0106** (2001) 063, arXiv:hep-th/0105132.

49. P. Binetruy, C. Deffayet and D. Langlois, *Nucl. Phys. B* **565** (2000) 269, arXiv:hep-th/9905012.
50. P. Bowcock, C. Charmousis and R. Gregory, *Class. Quantum Grav.* **17** (2000) 4745, arXiv:hep-th/0007177.
51. R. Maartens, *Phys. Rev. D* **62** (2000) 084023, arXiv:hep-th/0004166.
52. J. Garriga and T. Tanaka, *Phys. Rev. Lett.* **84** (2000) 2778, arXiv:hep-th/9911055.
53. T. Shiromizu, K.-I. Maeda and M. Sasaki, *Phys. Rev. D* **62** (2000) 024012, arXiv:gr-qc/9910076.
54. M. Sasaki, T. Shiromizu and K.-I. Maeda, *Phys. Rev. D* **62** (2000) 024008, arXiv:hep-th/9912233.